Fluid-Fluid Transitions at Bulk Supercritical Conditions

Xie, Fei; Woodward, Clifford E.; Forsman, Jan

Published in:
Langmuir

DOI:
10.1021/la400248m

2013

Fluid-fluid transitions at bulk supercritical conditions

Fei Xie*, Clifford E. Woodward** and Jan Forsman**

*Theoretical Chemistry, Chemical Centre, P.O.Box 124, S-221 00 Lund, Sweden

*School of Physical, Environmental and Mathematical Sciences, University of New South Wales,Canberra Canberra ACT 2600, Australia

E-mail: fei.xie@teokem.lu.se

Abstract

We use three different polymer solvent mixture models to theoretically determine the existence of capillary induced phase separation in simple pores under supercritical bulk conditions. These models undergo bulk demixing, due to quite different mechanisms, yet readily display supercritical transitions without the use of esoteric interactions in the capillary. The theoretical method used to analyze these systems is density functional theory. We find that capillary demixing is not reliant on the presence of of a pure surface transition, but may occur in the absence of the latter. This is shown by considering cases where the surface enhancement factor is too weak to cause demixing at a single surface, or else the bulk conditions are supercritical to both bulk and surface transitions. This phenomenon may prove useful in applications involving adsorption from mixtures into porous particles.

Introduction

It it well-known that fluids at surfaces or in narrow spaces, such as small pores (capillaries), usually display phase behaviours that differ from those in the bulk.[1–7] The presence of surfaces leads

*To whom correspondence should be addressed

to a truncation of the range of intermolecular potentials, thus weakening fluid-fluid interactions adjacent to them. In a pore, weakening of fluid interactions has a similar impact on the phase diagram that an increased temperature has in the bulk. In other words, in narrow spaces,[4,6] an upper critical temperature is generally lower than in the bulk.

In this work, we shall explore the more rare situations wherein surfaces effectively induce a strengthening of fluid-fluid interactions. At a single surface it has been shown that, when the surface enhancement parameter, J, is above a critical value, J_c, this may give rise to a *surface transition* which is essentially equivalent to first-order surface wetting, albeit under possibly supercritical conditions.[1] As with wetting, the surface transition has a critical temperature, which we denote by T_{sc}. Here we shall focus our study on narrow pores where wetting would normally be superseded by capillary induced phase separation (CIPS).[8] Thus, by analogy with the behaviour at a single surface, a pore may destabilize the confined fluid, giving a CIPS, even while the bulk is supercritical. For strong surface enhancement ($J > J_c$), surface demixing at supercritical temperatures will persist as the pore radius becomes infinitely large. For those situations where a single surface transition is not observed, e.g., $J < J_c$ or $T > T_{sc}$ a pore may still give rise to capillary demixing, due to the negative curvature of the pore geometry. As the pore size increases, this effect is weakened and at some point capillary demixing will cease at any supercritical temperature.

The models we will use in this study are binary mixtures, where one of the components is a polymer. In two of the models, the system displays a lower critical solution temperature (LCST) in the bulk. An LCST is more a rule than an exception for polymer solutions,[9–19] due to mechanisms such as the differential compressibility of solute and solvent or specific (non-isotropic) interactions, such as hydrogen bonds. We believe that this study will have significant potential for practical applications of real mixtures of this type. For instance, the enrichment of one component within the capillaries of a porous adsorbate in a supercritical binary bulk mixture would be an interesting option for continuous-flow processes, where global phase separation might be undesirable. We shall also investigate an athermal model, which displays a lower critical *pressure*, due to depletion interactions between monomers, induced by the solvent. This system illustrates a fundamental

mechanism that may be of importance in polymer solvent mixtures, wherein the monomer size is larger than that of the solvent.

The idea that an LCST might be lowered in a heterogeneous environment is not entirely new. Kotelyanskii and Kumar[20] performed simulations on a lattice model of a simple binary A-B mixture, interacting through a combination of isotropic and directional (hydrogen bond) potentials. Their results did suggest that the capillary critical temperature was slightly below the corresponding bulk value, though their data was rather noisy (which is to be expected close to a critical point). The work of Kotelyanskii and Kumar suggests that this phenomenon is somewhat "special" and that similar behaviour would not likely be obtained for fluids without anisotropic interactions. However, the study presented here will demonstrate that fluid instabilities in pores can occur when the bulk solution is well inside the supercritical regime, and all interactions are isotropic.

Our work uses classical density functional theory (DFT), which allows us to accurately model capillary coexistence at temperatures below the bulk LCST. As mentioned above, we will investigate three *very* different polymer solution models, all of which display capillary-induce phase separation for a bulk fluid well inside the supercritical regime. These are described in detail in the next section, but their main features can be summarized as follows:

- Model I. This model is designed to mimic non-aqueous polymer solutions, i.e., those with relatively weak isotropic interactions. Such solutions are known to display a demixing region with an LCST, which is primarily driven by a difference in compressibility between the polymer fluid and the solvent. For this reason, the mixture can become unstable around the critical temperature of the pure solvent, which will usually be well below that of the neat polymer. At higher temperatures there is a reentrant miscible phase. A specific example is a polystyrene-toluene mixture.[21] In these rather highly compressible systems, demixing is favoured by a low pressure and tends to vanish at high pressures.

- Model II. This models a dense (essentially incompressible) polymer solution, wherein the interactions between monomers and the solvent are dependent upon the value of an internal state variable of the monomers, As with hydrogen bonds, we assume the average interaction

is entropically weakened at high temperatures. Thus, demixing may result if the temperature increases. A classic example of this type of system is poly(ethylene oxide) - water (PEO-water).

- Model III. This model differs considerably from the other two in that it is strictly athermal, i.e., excluded volume considerations alone govern the phase behaviour. Here, the solvent particles are smaller than monomers, and demixing is promoted by *high* pressures.[22–24] In this system, we will demonstrate that CIPS may occur between simple hard surfaces at pressures substantially below the bulk critical value. This model essentially isolates excluded volume effects in dense systems, with a size disparity between solvent and monomers. Being purely athermal, it lacks a direct experimental analogue, but it nevertheless highlights a mechanism which may be quite relevant in many liquid solutions.

These three model systems will be shown to exhibit a CIPS, even when the bulk solution, with which the confined solution is in is equilibrium, is supercritical. Furthermore, in many cases demixing persists for rather wide pores (and even single surfaces) at ambient conditions relatively far from the critical point. This suggests that experimental verification of these phenomena are feasible and that practical applications can be useful over a wide range of conditions.

Theory and models

We shall use versions of the polymer DFT, originally developed by Woodward,[25] to predict the behaviours of our various models. Consider a polymer made up of r monomers. Denoting the coordinate of monomer i by $\mathbf{r}_i$, we can represent a polymer configuration by $\mathbf{R} = (\mathbf{r}_1, ..., \mathbf{r}_r)$. We introduce a multi-point density distribution $N(\mathbf{R})$, such that $N(\mathbf{R})d\mathbf{R}$ is the number of polymer molecules having configurations between $\mathbf{R}$ and $\mathbf{R} + d\mathbf{R}$. The monomers along a chain are connected by bonds, described by the bonding potential $V_b(\mathbf{R})$. In this study, we will only consider bonds of fixed length, but without angular constraints, i.e.: $e^{-\beta V_b(\mathbf{R})} \propto \prod \delta(|\mathbf{r}_{i+1} - \mathbf{r}_i| - \sigma)$ where σ is the bond length, $\delta(x)$ is the Dirac delta function, and $\beta = 1/(k_B T)$ is the inverse thermal

energy.

For a completely ideal polymer solution, in which there are no particle-particle interactions or external fields, save the bond constraints, the polymer free energy, $\mathscr{F}_p^{id}$, can be *exactly* written as:

$$\beta\mathscr{F}_p^{(id)} = \int N(\mathbf{R})\left(\ln[N(\mathbf{R})]-1\right)d\mathbf{R} + \beta\int N(\mathbf{R})V_b(\mathbf{R})d\mathbf{R} \tag{1}$$

In the presence of an ideal (point-particle) solvent, and external fields, the functional, $\mathscr{F}^{(id)}$ is still exact:

$$\beta\mathscr{F}^{(id)} = \beta\mathscr{F}_p^{(id)} + \int n_s(\mathbf{r})\left(\ln[n_s(\mathbf{r})]-1\right)d\mathbf{r} + \beta\int (n_m(\mathbf{r})V_{ex}^{(m)}(\mathbf{r}) + n_s(\mathbf{r})V_{ex}^{(s)}(\mathbf{r}))d\mathbf{r} \tag{2}$$

where $n_m(\mathbf{r})$ and $n_s(\mathbf{r})$ are the monomer and solvent densities, while $V_{ex}^{(\alpha)}$ are external potentials, acting on these particles (i.e. "α = m or s"). In DFT, interparticle interactions are usually approximated by an additional "excess" term, $\mathscr{F}^{(ex)}[n_m(\mathbf{r}),n_s(\mathbf{r})]$. This is added to the ideal free energy to give the total free energy $\mathscr{F}$. It is convenient to divide the excess free energy into one excluded volume (hard-sphere) term, $\mathscr{F}_{HS}^{(ex)}[n_m(\mathbf{r}),n_s(\mathbf{r})]$ and a separate term, $\mathscr{U}[n_m(\mathbf{r}),n_s(\mathbf{r})]$ describing attractive interaction energies. Finally, equilibrium between the pore regime and the surrounding bulk solution is ensured via the polymer and solvent chemical potentials, μ_p and μ_s, and the total grand potential, Ω, has the following general appearance:

$$\Omega = \mathscr{F}^{(id)} + \mathscr{F}_{HS}^{(ex)} + \mathscr{U} - \mu_s\int n_s(\mathbf{r})d\mathbf{r} - \mu_p\int n_m(\mathbf{r})d\mathbf{r} \tag{3}$$

The exposition thus far is quite general. The three models to be investigated correspond to different choices of $\mathscr{F}^{(ex)}[n_m(\mathbf{r}),n_s(\mathbf{r})]$, and the applied potential, $V_{ex}^{(\alpha)}$. The "capillary" is modelled by two parallel surfaces, with area S, located at $z=0$ and h. In essence, we allow the area S to approach infinity and the inherent mean-field nature of our theory allows us to integrate over the x,y plane, without loss of information. This simplifies the free energy, making it a functional of the density distributions along the z axis. The external field can be written as a sum of single-wall

contributions: $V_{ex}^{(\alpha)}(z) = w^{(\alpha)}(z) + w^{(\alpha)}(h-z)$. In this planar geometry, we can relate the free energy Ω to the average of pressure tensor component parallel to the surfaces $p_{||}(z)$. The average is over the pore width:

$$< p_{||} >= \frac{1}{h}\int_0^h p_{||}(z) \tag{4}$$

The average pressure tensor, $< p_{||} >$, plays an analogous role in a pore, as the pressure in the bulk. That is, while h is fixed, the natural volume fluctuations occur parallel to the surfaces. Furthermore, for phase coexistence in the pore one requires equivalence between the individual chemical potentials and $< p_{||} >$ in both phases. The latter requirement is equivalent to requiring the same value of the free energy per unit area, Ω/S, as is obvious from the relation:

$$\Omega = - < p_{||} > hS \tag{5}$$

Armed with this general formalism, we now provide the specific details for each of the models.

Model I

Here we model polymer solutions where non-polar interactions dominate. In order to reduce the number of parameters, we will restrict ourselves to the simple "polymer dissolved in monomers" model. That is, the spherical solvent particles, with diameter σ, are identical to the monomers that are connected to form a chain (a close experimental analogue would be a polystyrene-tolouene mixture). All particles mutually interact via a hard sphere + Lennard-Jones potential. The hard-sphere interaction has a range σ, so the interaction energy term of the grand potential functional, 3, can be written as:

$$\mathscr{U}[n_m(\mathbf{r}), n_s(\mathbf{r})] = \frac{1}{2}\sum_{\alpha\beta}\int\int n_\alpha(\mathbf{r}) n_\beta(\mathbf{r}) \phi^{(a)}(\mathbf{r},\mathbf{r}') d\mathbf{r}' d\mathbf{r} \tag{6}$$

where $\phi^{(a)}$ is the attractive part of the Lennard-Jones potential:

$$\begin{aligned} \phi^{(a)}(r) = &\quad 4\varepsilon((\tfrac{\sigma}{r})^{12} - (\tfrac{\sigma}{r})^{6}) \quad \text{r} > \sigma \\ = &\quad 0 \qquad\qquad \text{otherwise} \end{aligned} \tag{7}$$

where ε measures the maximum potential depth.

The bulk phase behaviour of this model has been rather thoroughly investigated in previous works.[14,15,17] Depending on the model parameters, this system may undergo demixing, typically displaying a closed-loop liquid-liquid coexistence curve. However, by changing the pressure and/or the polymer length, other kinds of phase diagrams (e.g., hour-glass shaped etc.) may be predicted. The demixing is primarily caused by a difference in compressibility between the solvent and the polymers. Normally, the driving force for mixing can be found in the ideal term of the free energy. However, when the compressibility of the solvent (non-polymer) component becomes large, the polymer solution mixing entropy may become negative and the liquid-liquid phase separation ensues. As monomers are unable to exploit "free volume" in the same manner as the solvent particles, there is a significant reduction in the free volume when the components are mixed. It occurs at pressures and temperatures where the pure solvent would be a vapour.

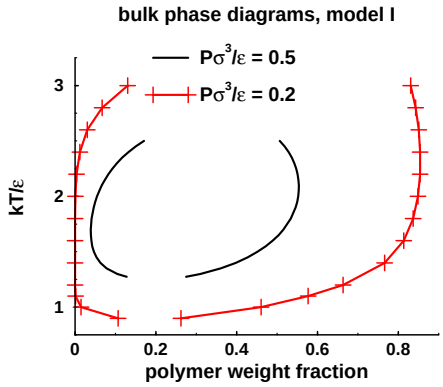

Figure 1: Model I bulk phase diagrams, at two different pressures. The higher pressure is used for the capillary phase investigations.

The excluded volume term, $\mathscr{F}_{HS}^{(ex)}$, is estimated by integrating the generalized-Flory equation

of state.[26,27] Detailed expressions are provided in earlier work.[27] We shall specifically investigate 20-mers, and examples of bulk phase diagrams, at two different pressures, are given in Figure 1. Note that other equations of state for polymer solutions (aside from GFD), such as those suggested by Song et al.,[28] or by Yu and Wu,[29] will predict similar phase behaviours for this type of system ("polymers in monomers").

In our current study, the solvent-surface interaction, $w^{(s)}$, results from a half-space of cubically close-packed L-J particles, interacting with the fluid. That is:

$$w^{(s)} = 2\pi\sigma^3\varepsilon_w \left[\frac{2}{45}\left(\frac{\sigma}{z+\frac{\sigma}{2}}\right)^9 - \frac{1}{3}\left(\frac{\sigma}{z+\frac{\sigma}{2}}\right)^3 \right] \tag{8}$$

where we have set $\varepsilon_w = 0.5\varepsilon$. The expression for the monomer-surface potential is similar, though here we introduce a variable parameter, γ:

$$w^{(m)} = 2\pi\sigma^3\varepsilon_w \left[\frac{2}{45}\left(\frac{\sigma}{z+\frac{\sigma}{2}}\right)^9 - \frac{\gamma}{3}\left(\frac{\sigma}{z+\frac{\sigma}{2}}\right)^3 \right] \tag{9}$$

γ is used to regulate the nature of the surface interaction with the monomers, either adsorbing or non-adsorbing. In this work, an adsorbing surface is characterized by $\gamma = 2$, whereas $\gamma = 1$ defines a non-adsorbing surface.

Model II

Here, we aim to model an essentially incompressible polymer solution in which the interactions are strong. In aqueous solutions, this will likely include strongly dipolar interactions and/or hydrogen bonds combined with dispersion forces, as, for example, in aqueous solutions of poly(ethylene oxide). A simple and physically appealing model for the PEO-water system was proposed by Karlström.[11] He suggested that the LCST is related to the possibility for the monomers to switch between two states (trans-gauche), one of which is polar, with subsequently stronger solvent interactions compared to the other, which is non-polar. The non-polar state has the larger intrinsic entropy and was thus favoured at higher temperatures. This mimics the diminishing hydrogen

bonding that occurs at higher temperature. While we will borrow from these concepts, our model is more generic. Thus, we shall simply name the monomers states "A" and "B", with degeneracies g_A and g_B, respectively. Furthermore, the functional is generalized to account for the state probabilities. The presence of monomer states leads to additional terms in the free energy functional (as described below). In order to remove compressibility effects, we shall assume that the total density of monomers+solvent particles is fixed to the constant value, n_t, at every point in space. This kind of model, which resembles the Scheutjens-Fleer theory[30] (albeit within a continuum space description), was introduced by us in earlier work.[31] The incompressibility constraint, $n_t = n_m(\mathbf{r}) + n_s(\mathbf{r})$, allows us to treat the solvent implicitly, i.e., the free energy functional, $\mathscr{F}$, can be expressed in terms of only the monomer densities and their state probabilities, P_α, (α = A,B). Thus:

$$\begin{aligned}\beta\mathscr{F} &= \beta\mathscr{F}_p^{(id)} + \int (n_t - n_m(\mathbf{r}))\ln[1-(n_t-n_m(\mathbf{r}))]\,d\mathbf{r} + \beta\mathscr{U}[n_m(\mathbf{r}),P_A(\mathbf{r})] + \\ &\int n(\mathbf{r})(1-P_A(\mathbf{r}))\ln\left[\frac{1-P_A(\mathbf{r})}{g_B}\right]d\mathbf{r} + \int n(\mathbf{r})P_A(\mathbf{r})\ln\left[\frac{P_A(\mathbf{r})}{g_A}\right]d\mathbf{r} + \\ &\beta\int (n_m(\mathbf{r})P_A(\mathbf{r})V_{ex}^{(A)}(\mathbf{r}) + n_m(\mathbf{r})(1-P_A((\mathbf{r}))V_{ex}^{(B)}(\mathbf{r}) + (n_t-n_m(\mathbf{r}))V_{ex}^{(s)}(\mathbf{r}))d\mathbf{r} \quad (10)\end{aligned}$$

where $V_{ex}^{\alpha}(\mathbf{r}))$ is the external (surface) potential acting on monomers in the α state. All particles, i.e. monomers and solvent, interact via attractive L-J potentials, but contrary model model I, these have in general different strengths:

$$\phi_{\alpha\beta}^{(a)}(r) = 4\varepsilon_{\alpha\beta}((\frac{\sigma}{r})^{12} - (\frac{\sigma}{r})^{6}), \qquad r > \sigma \quad (11)$$

where α and β denote either monomers states (A,B) or solvent particles, s. The energy functional is similar in form to 6, but we now need to consider the different monomer states, and interaction strengths:

$$\mathscr{U}[n_m(\mathbf{r}),P_A(\mathbf{r})] = \frac{1}{2}\sum_{\alpha,\beta}\int\int n_\alpha(\mathbf{r})n_\beta(\mathbf{r}')\phi_{\alpha\beta}^{(a)}(|\mathbf{r}-\mathbf{r}'|)d\mathbf{r}'d\mathbf{r} \quad (12)$$

where we have defined $n_A(\mathbf{r}) \equiv n_m(\mathbf{r})P_A(\mathbf{r})$ and $n_B(\mathbf{r}) \equiv n_m(\mathbf{r})(1-P_A(\mathbf{r}))$. In principle, there are six different sets of parameters for the L-J inter-particle potentials. Due to the incompressibility

constraint and the arbitrariness of the energy zero (the latter serves to shift the chemical potential) only four are independent. Here, we further simplify the model by setting several of these to a common value. Using an arbitrary energy scale ε_{ss}, we can define the reduced temperature $T* = kT/\varepsilon_{ss}$. In units of ε_{ss}, we have set $\varepsilon_{ss} = \varepsilon_{AA} = \varepsilon_{As} = 1$ and $\varepsilon_{BB} = \varepsilon_{Bs} = 0.3$ while $\varepsilon_{AB} = \sqrt{0.3}$ In addition, the monomer state degeneracies are $g_A = 1$, and $g_B = 12$, and the number of monomers in each polymer (r) is 200. The functional was then minimized with respect to $n_m(\mathbf{r})$ as well as $P_\alpha(\mathbf{r})$. The bulk solution of this system displays a demixing regime, with a lower critical temperature of $T^*_{LCST} = 2.8007$. The bulk phase diagram is shown in Figure 2. For the case of the confined fluid the

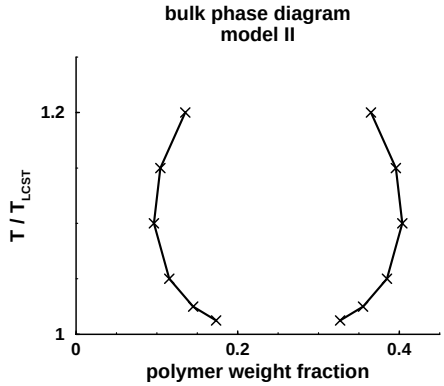

Figure 2: Bulk phase diagram for model II.

presence of the walls induces an effective surface potential, which disfavours A species more than B. This is because A species are better solvated and thus pay a higher free energy in moving from the bulk into the interstitial regions. In addition, we assume the presence of a direct interaction between the walls and the fluid particles, which has the following hard core+LJ form:

$$w^\alpha(z) = \begin{cases} \varepsilon_{w\alpha}\left[\frac{\sigma}{z+\frac{\sigma}{2}}\right]^3, & \frac{\sigma}{2} \le z \le h - \frac{\sigma}{2} \\ \infty, \quad z < \frac{\sigma}{2}, & z > h - \frac{\sigma}{2} \end{cases} \tag{13}$$

where $\varepsilon_{w\alpha}$ measures the interaction strength between the surface and the species α. Unlike our analysis of model I, we shall only investigate a single choice of parameter set for the surfaces. They are, $(\varepsilon_{wA} - \varepsilon_{ss})/T_{LCST}* = 1.5$, $(\varepsilon_{wB} - \varepsilon_{ss})/T_{LCST}* = 0.5$ and $(\varepsilon_{ws} - \varepsilon_{ss}) = 0$. This potential

serves to repel A species relative to B species.

Model III

In this model, we also consider a polymer solvent mixture, wherein the constituent particles are hard spheres, with the solvent particle *diameter* assumed to be half that of a monomer. Thus, unlike the previous two models, this system is athermal. It has been thoroughly described by us in previous work,[23,24] so we will only summarize the main features here.

We consider the bulk first. In a solvent-dominated solution, at sufficiently high pressures, monomers will effectively attract each other, via a solvent-mediated potential of mean force. This potential of mean force is attractive and due to a depletion interaction between monomers. Concentrating the monomers will increase the free volume available to the solvent. Thus, there is a mechanism for fluid-fluid demixing. The range of pressures for which bulk demixing exists, depends on the polymer length. Here we shall consider 175-mers. Previous studies for this system in the bulk and at single surfaces can be found in an earlier reference.[32] We again use the Generalized Flory-dimer approach to treat the hard-sphere (excluded volume) contributions to the free energy functional. The bulk phase diagram is shown in Figure 3, where we plot pressure versus reduced monomer density. Note that a closed-loop coexistence curve is not observed, as the system continues to display phase coexistence as the pressure is increased. Thus, unlike the previous two models, there is just a single "lower" critical point. Nevertheless, we will also demonstrate that in this system, one may observe phase transitions in capillaries under supercritical bulk conditions.

For this model, the capillary surfaces consist of simple hard walls. In our previous studies,,[24] we showed that the presence of a single surface can induce a surface surface transition, substantially below the bulk critical pressure. This is also shown in Figure 3. The surface transition is driven by an enhanced monomer-monomer interaction close to the surface, where the solvent concentration is high. Another way of understanding this phenomenon is the region proximal to the surface, the average parallel component of the pressure tensor, is higher than the bulk pressure. Thus, demixing in the proximal region is enhanced. When two such surfaces form a narrow cap-

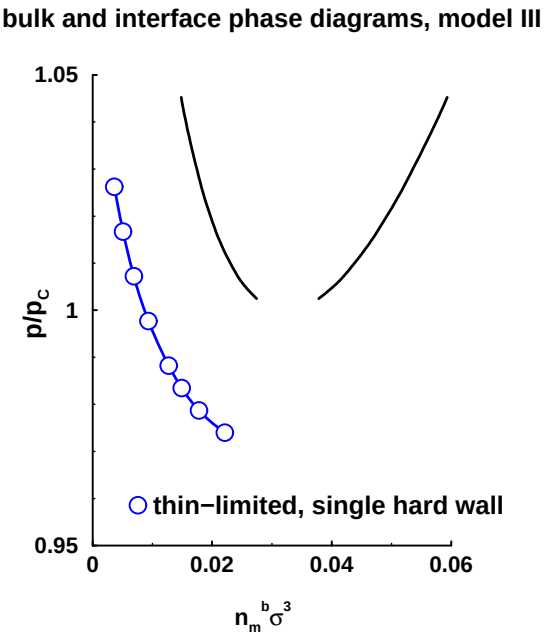

Figure 3: Bulk phase diagram for model III. The bulk pressure is denoted p, with a bulk critical value p_C. Circles show points of coexistence, between "thin" and "limited" single surface phases (cf. ref.[24] for details).

illary, this effect is even stronger, and demixing occurs deep within the supercritical regime, as compared with a single isolated surface (see below).

Results

We will report various density profiles, and capillary coexistence diagrams, as displayed by our different models. In all the cases we discuss the bulk solution is supercritical.

Model I

In this system, the solvent consists of similar kinds of particles to the monomers. Thus, standard Flory-Huggins theory would predict complete miscibility for all concentrations. The origin of this erroneous prediction is that the Flory-Huggins model fails to account for compressibility effects, which are of crucial importance to the phase behaviour of these systems. In the presence of sur-

faces, we find that interparticle interactions between fluid particles are truncated, which may have a profound effect on the phase behaviour. As stated earlier, for a simple fluid with an upper critical temperature the interaction truncation will lower the critical temperature of the confined liquid. For the *fluid mixture* in Model I, the effects are more complex, due to the interaction between solvent and polymer. In particular, we find that the fluid in a capillary displays a LCST, which is significantly lower that the bulk value. This is consistent with the behaviour of the pressure tensor component, acting parallel with the surfaces, $< p_{||} >$, which is generally lower than the bulk pressure at coexistence. That is, we know that lowering the pressure in Model I fluid leads to a lowering of the LCST of the bulk solution. We now consider in detail the behaviour of the system for different types of surfaces.

Adsorbing surfaces, $\gamma = 2$

At relatively low bulk concentrations, we may in this case observe CIPS in narrow capillaries, wherein narrow pores become polymer-enriched, i.e. filled with a concentrated phase. In Figure 4,

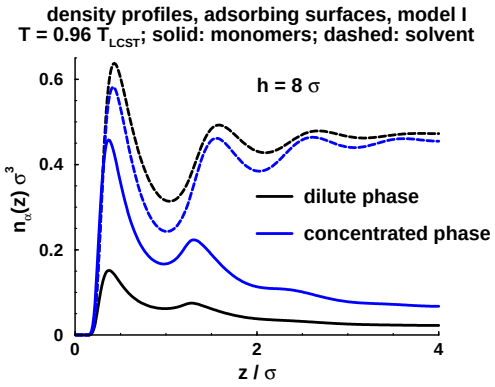

Figure 4: Density profiles, for coexisting dilute and concentrated phases (model I), in a capillary with monomer-adsorbing surfaces ($\gamma = 2$).

we give examples of density profiles, for dilute and concentrated capillary phases. Specifically, these have been obtained at a temperature four percent below the bulk LCST.

Figure 5 shows the excess monomer adsorption (beyond the bulk), Γ for coexisting phases as a

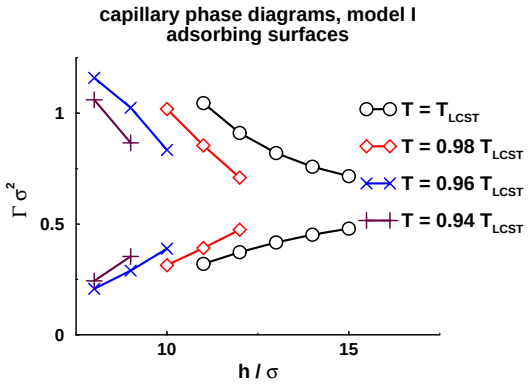

Figure 5: Capillary phase diagrams, for model I, with adsorbing surfaces ($\gamma = 2$). Γ is the excess monomer adsorption.

function of surface separation, for a range of temperatures. The excess adsorption is given by:

$$\Gamma = \int_0^h dz[n_m(z) - n_{bulk}] \tag{14}$$

where $n_m(z)$ is the monomer density at point z in the pore, and n_{bulk} is its bulk value. The presence of surfaces, which are attractive to the polymer mean that the adsorption excess, Γ, (with respect to the bulk) is positive. We clearly see capillary-induced demixing at temperatures well below the bulk LCST. The coexisting phases within the capillary merge together at some critical separation, h_c, the value of which increases with temperature. It appears that this system does not display a transition at a single surface, for the chosen parameters. Thus, for $T = T_{LCST}$, $h_c \to \infty$. For pore separations below about $h = 10\sigma$ (roughly $5nm$, for typical monomer sizes), demixing persist more than 5 percent below the bulk LCST, which in typical cases corresponds to more than $20K$. Thus, the effect is expected to be measurable, and of practical significance. The reason why demixing occurs at supercritical conditions in the capillary is due to the truncation of the particle-particle interactions due to the presence of the surfaces. The lowering in binding energy causes the solvent in the capillary is more compressible than that in the bulk, at the same temperature. We recall that demixing in this system occurs when the solvent compressibility becomes high. This leads to a phase separation in the confined solution at temperatures below that at which the bulk would

demix. At a fixed separation the solution becomes critical as the temperature is lowered.

Non-adsorbing surfaces, $\gamma = 1$

In this case, the attractive surface potential is insufficient to give rise to a positive excess adsorption of the polymer molecules. Instead the polymer is depleted relative to the solvent particles, and Γ is negative. The resulting capillary phase diagram is given in Figure 6. The driving force for phase separation is the same as that for the case of adsorbing surfaces, above. However, the demixing regime seems remarkably independent of temperature. That is, the Γ values for concentrated and dilute phases do not vary significantly with temperature. In the bulk, as the temperature increases the propensity for demixing increases, as does the difference in the monomer concentrations of the two phases. In the presence of depleting surfaces, the excess adsorption of the dilute phase is very low and therefore not expected to decrease much further, even as the temperature is increased. In the concentrated phase, one expects the adsorption should increase with temperature, due to stronger interactions between polymers. However, increasing temperature also enhances the depletion effect of the surfaces, thus countering the expected increase in Γ.

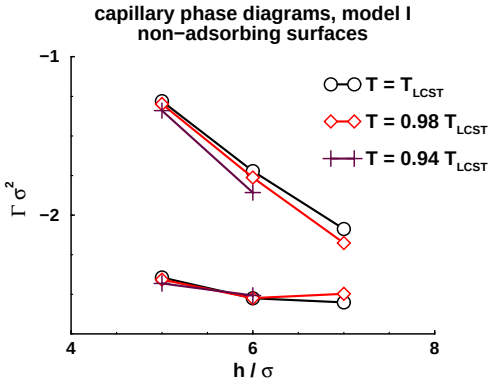

Figure 6: Capillary phase diagrams, for model I, with non-adsorbing surfaces ($\gamma = 1$).

Surface Forces

It might be of interest to briefly recapitulate the dramatic impact such transitions would have on the forces between any particles which may be dispersed in such a polymer solution.[8]

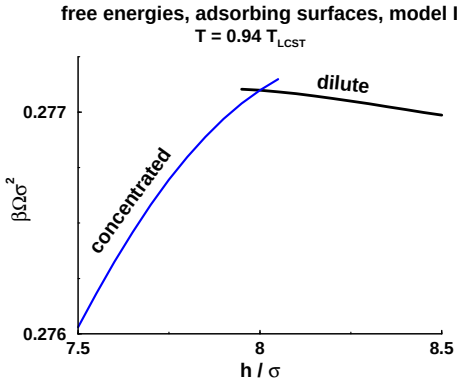

Figure 7: Interaction free energies for the model I system, with adsorbing surfaces, at $T = 0.94T_{LCST}$. The dilute and concentrated free energy branches crosses at some threshold separation, below which the latter phase is more stable. The crossing to a concentrated phase is accompanied by a strongly attractive interaction.[8]

An example is given in Figure 7, where we see how the slope of the equilibrium grand potential, i.e. the force, changes discontinuously as the separation is reduced to a value where a dilute to concentrated transition occurs. The impact on the behaviour of a say a *colloid/polymer solution* mixture under conditions that would initiate such a surface-surface phase transition will be a subject for future study.

Model II

In this model, we recall that "state A" monomers are effectively repelled (relative to other particles) by the surfaces, in this case. This is clearly reflected by the monomer densities shown in Figure 8. Here we again observe dilute and concentrated phases coexisting in a pore, at a temperature considerably below the bulk LCST ($T = 0.96T_{LCST}$). In fact, test calculations reveal that this system displays a supercritical single surface transition. While interesting, such a surface transition are not the main focus of this work.

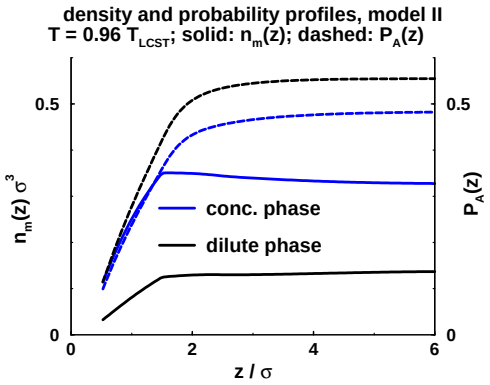

Figure 8: Coexisting monomer and A-state probability profiles, at $T = 0.96T_{LCST}$ (model II). The bulk monomer density is $n_m\sigma^3 = 0.339$.

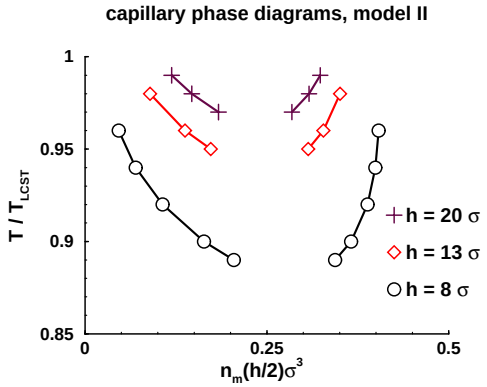

Figure 9: Capillary phase diagrams, for model II. The mid-plane monomer density of coexisting phases is shown, for various temperatures and slit widths.

In Figure 9, we display phase diagrams for pores of different widths. Given the behaviour of the model at a single surface, we note that the phase coexistence curves in Figure 9, will approach a limiting curve as h increases. This limiting curve describes the single surface phase transition. As the slit width becomes narrower, demixing progresses more deeply into the supercritical regime. For example, with $h = 8\sigma$, the capillary critical temperature is more than 10 percent below the bulk LCST.

In this model, the system displays a LCST in the bulk because of the of the higher intrinsic entropy of the B-state monomers, which are also less attractive to the solvent. Recall that we have the following degeneracies, $g_A = 1$ and $g_B = 12$. As the temperature is increased, so does

the population of B state monomers. This decreases the solubility of the polymer and gives rise to demixing. Further, increasing the temperature will essentially see the entropy of mixing assert itself and the polymer becomes miscible again, forming a closed loop demixing region. In the pore, the B-state is also more favoured than the A-state (relative to the bulk), due to the excluding effect of the walls and a surface potential that is more attractive to B-state monomers. Thus, the capillary acts to weaken polymer-solvent interactions, and enhances demixing, even for temperatures below the LCST of the bulk.

The lowering of the critical temperature in pores, observed in this study, would correspond to approximately 40-50 K for many polymer solutions. Though the potential parameters used here were not chosen to mimic any particular experimental system, our results show that this effect can be sizeable suggesting that it may find experimental support in the near future.

Model III

Model III is an athermal system, so the bulk phase behaviour can be visualized in pressure - composition space. That is the pressure plays the traditional role of temperature. In this respect this model has a "normal" phase behaviour. with a single lower critical pressure, p_c. The system will always phase separate at pressures $p > p_c$. When this fluid is in contact with hard surfaces, we find preferential adsorption of monomers (solvent), due to the “extra” free volume that is subsequently available. This leads to a high average value of $p_{||}$ at the surfaces, and the enhance possibility of a demixing transition adjacent to the surface. As can be seen in Figure 3, the fluid indeed displays a surface transition. This transition is terminated at a critical point of about $0.97p_C$. Thus, we anticipate the possibility for a CIPS in the presence of pores with hard walls. This is indeed observed, and at bulk pressures substantially below the lower bulk critical value and, in fact, lower than the critical pressure of the surface transition. In other words, the critical bulk pressure is lower for CIPS in narrow pores, than its single surface transition correspondence.

In Figure 10, we show an example of dilute and concentrated phases, coexisting in a planar pore, at a pressure four percent below the bulk critical value. We see that the solvent molar ratio is

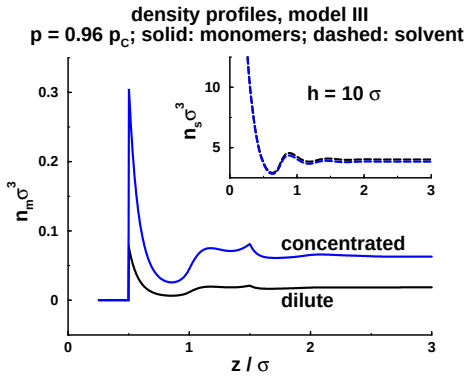

Figure 10: Coexisting concentrated and dilute density profiles, for model II, at $p = 0.96 p_C$. The main graph shows monomer densities, whereas the inset displays solvent profiles.

close to unity for both phases, but in relative terms, the monomer concentration is still considerably higher in the concentrated branch.

An example of a phase diagram, at a bulk pressure four percent below the bulk critical value, p_C, is presented in Figure 11.

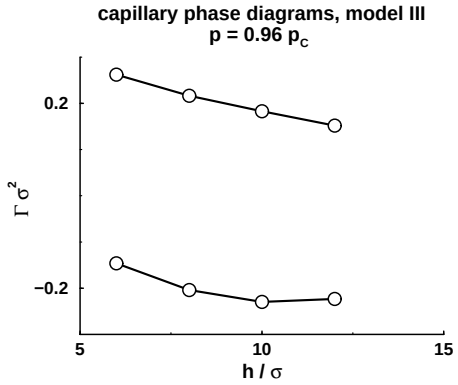

Figure 11: Capillary phase diagram, for model III, at $p = 0.96 p_C$. The excess adsorption of monomers, Γ, of coexisting phases are given, at various slit widths.

Conclusion

We have displayed supercritical CIPS in three different polymer solution models. These models undergo bulk demixing transitions, due to quite different mechanisms. Model I relies on significantly different compressibility between solvent and polymer. Model II displays different binding energy states between polymer and solvent. These binding states have different intrinsic entropy and a reduction in interaction between monomers and solvent is favoured at high temperatures. Finally, demixing in Model III uses the depletion interaction between monomers, due to the exclusion of solvent. This effect is larger at higher pressures. We have found that all these mechanisms can be enhanced when the fluid mixture is placed into pores, which can give rise to supercritical CIPS. Furthermore, three different scenarios are encountered in our studies, displaying different circumstances whereby CIPS can occur. In Model I, we investigated the case where the bulk was supercritical and the surface-fluid interaction was not sufficient to give rise to a transition at a single surface. In this case, the presence of two surfaces was still able to cause a supercritical transition in the pore. Presumably, this would be possible in all pores which display a negative curvature. For 0- or 1-dimensional cavities, however, the phase transitions would not be sharp. In the case of Model II, we considered a supercritical bulk and a surface interaction which was capable of giving rise to a single surface transition. Clearly, demixing occurs in a pore for this system, however, bulk behaviour is not recovered as the pore width becomes large. Finally, in Model III we considered the case whereby the system was supercritical with respect to both the bulk demixing and an existing single surface transition.

Rather than being "esoteric", this work shows that supercritical transitions, in pores can occur for relatively simple fluid mixtures with appropriate (but not elaborate) interactions. The effect is quite robust and can occur over a range of scenarios, albeit via a theory which is approximate. This notwithstanding, we believe that the qualitative aspects of the work presented here are essentially correct, though verification via simulations or, better still, experiment would be ultimately desirable. From a practical point of view this phenomenon may prove to be quite useful, especially in applications involving adsorption from mixtures into porous particles.

References

1. Nakanishi, H.; Fisher, M. E. Multicriticality of Wetting, Prewetting and Surface Transitions. *Phys. Rev. Lett.* **1982**, *49*, 1565–1568.

2. Lane, J. E.; Spurling, T. H. *Aust. J. Chem.* **1981**, *34*, 1529.

3. Evans, R.; Bettolo Marconi, M.; Tarazona, P. Fluids in narrow pores: Adsorption, capillary condensation, and critical points. *J. Chem. Phys.* **1986**, *84*, 2376.

4. Burgess, C. G. V.; Everett, D. H.; Nutall, S. Adsorption hysteresis in porous materials. *Pure & Appl. Chem.* **1989**, *61*, 1845–1852.

5. Forsman, J.; Woodward, C. E. Simulations of phase equilibria in planar slits. *Molec. Phys.* **1997**, *90*, 637.

6. Morishige, K.; Fujii, H.; Uga, M.; Kinukawa, D. Capillary Critical Point of Argon, Nitrogen, Oxygen, Ethylene, and Carbon Dioxide in MCM-41. *Langmuir* **1997**, *13*, 3494–3498.

7. Drzewiński, A.; Maciołek, A.; Barasiński, A.; Dietrich, S. Interplay of complete wetting, critical adsorption, and capillary condensation. *Phys. Rev. E* **2009**, *79*, 041145.

8. Wennerström, H.; Thuresson, K.; Linse, P.; Freyssingeas, E. Long Range Attractive Surface Forces Due to Capillary-Induced Polymer Incompatibility. *Langmuir* **1998**, *14*, 5664.

9. Kleintjens, L. A.; Koningsveld, R. Liquid-liquid phase separation in multicomponent polymer systems. *Coll. Polym. Sci. 258*, 711–718.

10. van Koynenburg, P. H.; Scott, R. L. Critical Lines and Phase Equilibria in Binary van der Waals Mixtures. *Phil. Trans. R. Soc. Lond. A* **1980**, *298*, 495.

11. Karlström, G. A new model for upper and lower critical solution temperatures in poly(ethylene oxide) solutions. *The Journal of Physical Chemistry* **1985**, *89*, 4962–4964.

12. Kleintjens, L. A. Developments in the thermodynamics of polymer systems. *Fluid Phase Equilibria* **1989**, *53*, 289–302.

13. Jackson, G. Theory of closed-loop liquid-liquid immiscibility in mixtures of molecules with directional attractive forc es. *Molecular Physics* **1991**, *72*, 1365–1385.

14. Luna-Barcenas, G.; Meredith, J. C.; Sanchez, I. C.; Johnston, K. P.; ov, D. G. G.; de Pablo, J. J. Relationship between polymer chain conformation and phase boundaries in a supercritical fluid. *The Journal of Chemical Physics* **1997**, *107*, 10782–10792.

15. Gromov, D. G.; de Pablo, J. J.; Luna-Barcenas, G.; Sanchez, I. C.; Johnston, K. P. Simulation of phase equilibria for polymer-supercritical solvent mixtures. *J. Chem. Phys.* **1998**, *108*, 4647.

16. Dormidontova, E. E. Role of Competitive PEO-Water and Water-Water Hydrogen Bonding in Aqueous Solution PEO Behavior. *Macromolecules* **2002**, *35*, 987–1001.

17. Paricaud, P.; Galindo, A.; Jackson, G. Understanding liquid-liquid immiscibility and LCST behaviour in polymer solutions with a Wertheim TPT1 description. *Molecular Physics* **2003**, *101*, 2575–2600.

18. Oh, S. Y.; Bae, Y. C. Role of intermolecular interactions for upper and lower critical solution temperature behaviors in polymer solutions: Molecular simulations and thermodynamic modeling. *Polymer* **2012**, *53*, 3772 – 3779.

19. Clark, E.; Lipson, J. LCST and UCST behavior in polymer solutions and blends. *Polymer* **2012**, *53*, 536 – 545.

20. Kotelyanskii, M.; Kumar, S. K. Surface Transitions for Confined Associating Mixtures. *Phys. Rev. Lett.* **1998**, *80*, 1252–1255.

21. Saeki, S.; Kuwahara, N.; Konno, S.; Kaneko', M. Upper and Lower Critical Solution Temperatures in Polystyrene Solutions. *Macromolecules* **1973**, *6*, 246–250.

22. Forsman, J.; Woodward, C. E.; Freasier, B. C. Density functional study of surface forces in athermal polymer solutions with additive hard sphere interactions: Solvent effects, capillary condensa tion, and capillary-induced surface transitions. *J. Chem. Phys.* **2002**, *117*, 1915–1926.

23. Forsman, J.; Woodward, C. E. Prewetting and layering in athermal polymer solutions. *Phys. Rev. Lett.* **2005**, *94*, 118301.

24. Forsman, J.; Woodward, C. E. Surface transition in athermal polymer solutions. *Phys. Rev. E,* **2006**, *73*, 051803.

25. Woodward, C. E. Density functional theory for inhomogeneous polymer solutions. *J. Chem. Phys.* **1991**, *94*, 3183.

26. Wichert, J. M.; Gulati, H. S.; Hall, C. K. Binary hard chain mixtures I. Generalized Flory equations of state. *J. Chem. Phys.* **1996**, *105*, 7669.

27. Forsman, J.; Woodward, C. E. Evaluating the accuracy of a density functional theory of polymer density functional theory of polymer solutions with additive hard sphere diameters. *J. Chem. Phys.* **2004**, *120*, 506.

28. Song, Y.; Lambert, S. M.; Prausnitz, J. M. Equation of state for mixtures of hard-sphere chains including copolymers. *Macromol.* **1994**, *27*, 441.

29. Yu, Y.-X.; Wu, J. Density functional theory for inhomogeneous mixtures of polymeric fluids. *J. Chem. Phys.* **2002**, *117*, 2368.

30. Scheutjens, J. M. H. M.; Fleer, G. J. Statistical theory of the adsorption of interacting chain molecules. 1. Partition function, segment density distribution, and adsorption isotherms. *J. Phys. Chem.* **1979**, *83*, 1619–1635.

31. Forsman, J.; Woodward, C. E. Surface forces in solutions containing rigid polymers: approaching the rod limit. *Macromol.* **2006**, *39*, 1269.

32. Forsman, J.; Woodward, C. E. Surface forces in solutions containing semiflexible polymers. *Macromol.* **2006**, *39*, 1261.

For Table of Contents Use Only